Development and validation of a mathematical model to simulate human cardiovascular and respiratory responses to battlefield trauma

Xin Jin, PhD[1,2], Srinivas Laxminarayan, PhD[1,2], Sridevi Nagaraja, PhD[1,2], Anders Wallqvist, PhD[1], and Jaques Reifman, PhD[1*]

[1]Department of Defense Biotechnology High Performance Computing Software Applications Institute, Telemedicine and Advanced Technology Research Center, United States Army Medical Research and Development Command, Fort Detrick, MD, USA
[2]The Henry M. Jackson Foundation for the Advancement of Military Medicine, Inc., Bethesda, MD, USA

Author e-mail addresses: X. Jin (xjin@bhsai.org), S. Laxminarayan (slaxminarayan@bhsai.org), S. Nagaraja (snagaraja@bhsai.org), A. Wallqvist (sven.a.wallqvist.civ@health.mil)

*Correspondence:
Jaques Reifman, Ph.D.
Senior Research Scientist
Director, Department of Defense Biotechnology High Performance Computing Software Applications Institute
Telemedicine and Advanced Technology Research Center
U.S. Army Medical Research and Development Command
ATTN: FCMR-TT, 504 Scott Street, Fort Detrick, MD 21702-5012
E-mail: jaques.reifman.civ@health.mil
Phone: + 1 301 619 7915
Fax: +1 301 619 1983

Short title: Model of human cardiovascular and respiratory responses to battlefield trauma

ABSTRACT

Mathematical models of human cardiovascular and respiratory systems provide a viable alternative to generate synthetic data to train artificial intelligence (AI) clinical decision-support systems and assess closed-loop control technologies, for military medical applications. However, existing models are either complex, standalone systems that lack the interface to other applications or fail to capture the essential features of the physiological responses to the major causes of battlefield trauma (i.e., hemorrhage and airway compromise). To address these limitations, we developed the cardio-respiratory (CR) model by expanding and integrating two previously published models of the cardiovascular and respiratory systems. We compared the vital signs predicted by the CR model with those from three models, using experimental data from 27 subjects in five studies, involving hemorrhage, fluid resuscitation, and respiratory perturbations. Overall, the CR model yielded relatively small root mean square errors (RMSEs) for mean arterial pressure (MAP; 20.88 mm Hg), end-tidal CO_2 (ETCO2; 3.50 mm Hg), O_2 saturation (SpO2; 3.40%), and arterial O_2 pressure (PaO2; 10.06 mm Hg), but a relatively large RMSE for heart rate (HR; 70.23 beats/min). In addition, the RMSEs for the CR model were 3% to 10% smaller than the three other models for HR, 11% to 15% for ETCO2, 0% to 33% for SpO2, and 10% to 64% for PaO2, while they were similar for MAP. In conclusion, the CR model balances simplicity and accuracy, while qualitatively and quantitatively capturing human physiological responses to battlefield trauma, supporting its use to train and assess emerging AI and control systems.

Keywords: cardiovascular system; mathematical model; respiratory system; trauma.

1. INTRODUCTION

The unprecedented survivability of U.S. combat casualties in the recent conflicts in Iraq and Afghanistan is attributed in part to the ability to evacuate casualties from the time of injury to a medical treatment facility in less than 60 minutes [1-3]. In future conflicts, where airspace is expected to be contested and casualty evacuation delayed, medics will need to provide field care with limited resources for hours, if not days [4]. More importantly, recent multi-domain military war games against a near-peer suggest that the U.S. military should be prepared to suffer a considerably larger number of daily casualties in future conflicts, which, together with prolonged field care, will overwhelm medics [5, 6]. Despite the drastic increase in casualty-to-medic ratio in this new paradigm, we expect that hemorrhage and airway compromise will continue to be the leading causes of potentially survivable death (~99%) on the battlefield [7].

One way to augment the capacity and capability of medics in such a scenario, and aid them in continuous casualty monitoring, triage, and treatment, is to rely on emerging autonomous or semi-autonomous systems, such as clinical decision-support systems based on artificial intelligence and closed-loop control systems [8-20]. However, to develop such artificial intelligence systems, we must have large amounts of clinical or experimental data, on the order of thousands of subjects [9], which is impractical. An alternative viable solution is to use well-validated, human physiology-based computational models to generate a comprehensive synthetic database of battlefield injuries and treatment solutions that reflect those of resource-limited, prolonged field-care environments. These models need to reproduce key aspects of human physiology associated with hemorrhage and airway compromise, the top two battlefield injuries, and generate vital-sign data that show both qualitative and quantitative agreement with clinical observations.

To develop mathematical models that effectively reproduce human responses to hemorrhage and airway compromise and the associated treatments, we must consider an integrated approach that represents both the cardiovascular and respiratory systems and accounts for their coupling [21-25]. Hemorrhage directly affects hemodynamics through the cardiovascular system, which in turn impairs blood flow to the lungs, interfering with gas exchange and reducing the function of the respiratory system [21, 22]. Similarly, airway compromise directly affects ventilation,

leading to hypoxia and hypercapnia, which in turn negatively impact the function of the cardiovascular system [23-25]. While many mathematical models have been developed to represent the cardiovascular and respiratory systems [26-41], the vast majority represent either the cardiovascular system [26-30] or the respiratory system [31-35], with only a few accounting for both [36-44]. Of these, most [36-42] cannot consider fluid perturbations characteristic of hemorrhage and fluid resuscitation because they do not have an interstitial fluid compartment to compensate for changes in blood volume [45], while others, such as the Pulse Physiology Engine [43] and the HumMod software [44], are standalone applications that lack the needed interface to other applications for the generation of a large database of synthetic casualties. In addition, these models are too complex, involving thousands of model parameters and variables [43, 44]. Importantly, except for the Pulse Physiology Engine [43], none of these models were specifically designed to capture the physiological responses caused by battlefield injuries (i.e., hemorrhage and airway compromise) and their associated treatments.

Here, we aimed to develop a human physiological model that balances simplicity and accuracy, while specifically capturing the essential features of the cardiovascular and respiratory responses to hemorrhage, fluid resuscitation, and respiratory perturbations, which are key for modeling the top two types of trauma-induced injuries on the battlefield. Accordingly, we developed the cardio-respiratory (CR) model by expanding and integrating two previously published works: Guyton's model [30] and Cheng et al.'s model [36]. To evaluate the performance of the CR model, we compared its predictions with three other models, referred to as Guyton, Cheng, and HumMod, using experimental data from five studies, involving hemorrhage, fluid resuscitation, and respiratory perturbations.

2. MATERIALS AND METHODS

2.1. Description of the Cardio-respiratory Model

To develop the CR model, we integrated Guyton's cardiovascular model and the fluid-shift mechanism described therein [30] with Cheng's respiratory model [36]. We coupled the two systems using an updated version of the coupling described in Cheng's model, to accommodate the simpler cardiovascular representation in Guyton's work (Figure 1). We incorporated the cardiovascular and respiratory dynamics, along with their regulatory mechanisms and couplings,

consisting of a system of 74 ordinary differential and algebraic equations and 74 parameters. We used a lumped-parameter formulation based on first principles (i.e., principles of mass conservation) to model the fluid balances within the vascular compartments and the gas balances within the lungs and tissues and a compartmental phenomenological formulation to represent the regulatory mechanisms and couplings. The CR model can simulate hemorrhage, fluid resuscitation, and respiratory perturbations, and predicts cardiovascular and respiratory vital signs under different conditions. We refer the reader to the Supplementary Material for a complete set of equations for the CR model (Text S1 in the Supplementary Material) and its associated parameters (Table S1 in the Supplementary Material) and coefficients (Table S2 in the Supplementary Material).

2.1.1. Cardiovascular model

The cardiovascular model, based on Guyton's work [30], includes mathematical descriptions for circulatory dynamics, the fluid shift between the circulatory and interstitial fluid compartments, the renal system, the sympathetic stimulation, and the angiotensin control mechanism (Figure 1, A). The model's inputs are the rates of hemorrhage or fluid resuscitation, and its outputs consist of time courses of four vital signs, mean arterial pressure (MAP), systolic blood pressure (SBP), diastolic blood pressure (DBP), and heart rate (HR). We obtained the circulatory dynamics by enforcing macroscopic mass balances for each vascular compartment, including the heart, arteries, and veins. We estimated SBP and DBP from empirical equations derived from HumMod [44] based on MAP and estimated HR based on the blood pressure of the right atrium and the regulatory effects of sympathetic stimulation on HR [Equations (S1)–(S32) in the Supplementary Material].

2.1.2. Respiratory model

The respiratory model, based on Cheng's work [36], consists of three compartments, representing gas storage and exchange in the lungs, brain tissue, and body tissue (Figure 1, C). The model's inputs are the minute ventilation (MV) and the fraction of inspired oxygen (FiO2), and its outputs are the partial pressure of end-tidal carbon dioxide (ETCO2) and oxygen saturation (SpO2). We obtained the respiratory dynamics by imposing macroscopic mass

balances in the lungs, brain tissue, and body tissue [Equations (S33)–(S49) in the Supplementary Material].

2.1.3. Coupling model

The coupling of the two models (Figure 1, B), adapted from Cheng's work and originally developed by Ursino and Magosso [23-25], describes how the cardiovascular and respiratory models interact via the central nervous system and local blood flow control [Equations (S50)–(S74) in the Supplementary Material]. The central nervous system includes the baroreceptor, chemoreceptor, lung stretch receptor, and central nervous system ischemic responses. Its inputs include the arterial O_2 (PaO2) and CO_2 pressures (PaCO2) from the respiratory model, while its outputs to the cardiovascular model include the central nervous system effects on the venous resistance and blood volume in the veins, heart contractility, and HR. The local blood flow control changes the venous resistance to regulate blood flow in the circulatory system of the cardiovascular model. Its inputs are the PaO2 and PaCO2, and its outputs are the local blood flow control effects on the venous resistance. We used the blood flow rates in the circulatory system to determine the blood flow rates through the brain and body tissues of the respiratory model.

2.2. Comparison of the Cardio-respiratory Model with Other Models

2.2.1. Models used for comparison

To assess the performance of the CR model, we compared and contrasted its predictions with three other models: Guyton's model [30], Cheng's model [36], and HumMod [44]. Guyton's model, which is a purely cardiovascular model, contains 22 parameters and can only simulate hemorrhage and fluid resuscitation. In contrast, Cheng's model contains ~200 parameters that characterize the respiratory, cardiovascular, and sleep-wake systems, and can simulate hemorrhage, fluid resuscitation, and respiratory perturbations. The more complex HumMod software consists of ~5,000 parameters and variables that describe and can be used to simulate dozens of conditions, such as food ingestion, anesthesia, and exercise.

2.2.2. Experimental studies

To assess the models, we used existing experimental data from five studies (Table 1). Briefly, Studies 1–2 involved nine Yorkshire and eight domestic pigs (weight: 35–45 kg), respectively, challenged with 78–150 minutes of hemorrhage (65% of blood volume), fluid resuscitation (25–35%), and respiratory perturbations (MV: 3.5–12.8 L/min, FiO2: 26–100%) [21, 46]. In contrast, Studies 3–5 involved a total of 46 human participants subjected to 25–34 minutes of respiratory perturbations (MV: 3.5–15.0 L/min, FiO2: 9–21%) [47-49]. Although not consistent across the studies, the measurements included vital signs and the rates of hemorrhage and fluid resuscitation. We refer the reader to the original articles for additional information.

2.2.3. Comparison procedure and metrics

To assess the performance of the CR model against the experimental data and the three other models, we simulated the experimental scenarios in each of the five experimental studies described in Section 2.2.2 using all four of the models to obtain the time courses of the vital signs. Because the experiments in Studies 1–2 were performed in animals and the four models were developed to represent humans, we normalized the experimental inputs (e.g., hemorrhage and resuscitation rates) before applying them to the models. To do this, we multiplied the inputs by the ratio of the average weight of the animals in each study to the weight of an average human (i.e., 70 kg [50]). In addition, once the simulations from all four of the models were complete, we also normalized the simulated outputs of the vital signs (i.e., MAP, HR, ETCO2, and SpO2). We did this because the experimental outputs as well as the simulated outputs from the models have different ranges, and normalizing the output values allowed for a head-to-head comparison. To do this, for all models, we multiplied each simulated output by the ratio of the initial mean value of the corresponding experimental measurement to the initial value of that specific model output. To quantitatively compare the performance of the different models, we calculated two metrics. First, we computed the root mean square error ($RMSE_k$) between the normalized output $\tilde{y}_k$ and the mean of experimentally measured value Z_k, for each vital sign k, as follows:

$$RMSE_k = \mathrm{norm}\left(\left[Z_k - \tilde{y}_k\right]/N\right) \quad (1)$$

where norm(·) denotes the Euclidean norm of a vector of length N, representing the number of experimental data points. Second, we computed the percentage of the normalized predicted output $\tilde{y}_k$ that fell within 95% of the confidence interval of the measured data $CI_k(t)$ at time t around Z_k, with

$$CI_k(t) = Z_k(t) \pm 1.96\sigma_k(t) \quad (2)$$

where $\sigma_k(t)$ represents the standard error of the mean of vital sign k at time t and 1.96 represents the standard score for a 95% confidence level [51]. We considered a model to be accurate if at least ~70% of its predictions fell within CI [52]. We compared these two metrics across the four models to assess their prediction performance.

2.3. Calibration of the Cardio-respiratory Model

To assess whether the predictions of the CR model could be improved, we calibrated the most sensitive model parameters to the means of the experimentally measured outputs from the nine subjects in Study 1. To identify these parameters, we first used the Latin hypercube sampling method [53] to generate 100 unique parameter sets, each representing a different "subject," by randomly selecting parameter values around ±50% of their nominal values. Using these 100 subjects, we performed a global sensitivity analysis and selected the top two or three most sensitive parameters for each model output, for a total of 10 parameters to calibrate (Text S2 and Table S3 in the Supplementary Material). To calibrate the parameters, we again used the Latin hypercube sampling method to generate 5,000 parameter sets for the 10 parameters, while using the nominal values for the other 64 model parameters. Then, using these parameter sets, we performed 5,000 simulations, where for each simulation we computed the sum of the normalized RMSEs (S_e) over the four model outputs and selected the parameter set with the lowest S_e as the final calibrated parameter values:

$$S_e = \sum_{k=1}^{4} \frac{RMSE_k}{Z_k^0} \quad (3)$$

In addition, to investigate whether the CR model could predict the outputs of individual subjects, we followed the same procedure and calibrated the CR model to reproduce the four model outputs for each of the nine subjects in Study 1. We only performed individualized calibration for Study 1 because subject data for the other studies were not available.

3. RESULTS

3.1. Comparison of the Four Models

To assess the performance of the CR model, we compared and contrasted its predictions with the three other models using the two metrics described in Section 2.2.3 (i.e., RMSE and prediction

accuracy) for experimental data from the five studies (Table 2, Figures 2–4, and Figures S1 and S2 in the Supplementary Material). However, not all of the models used in our comparisons were able to simulate every experimental scenario. For example, Cheng's model was unable to simulate severe hemorrhage while HumMod could simulate severe hemorrhage only when interspersed with fluid resuscitation. Moreover, Guyton's model was unable to simulate respiratory perturbations. In addition, each experimental study only reported the values of a subset of the vital signs predicted by the CR model. Therefore, not all predicted vital signs could be assessed in each study. Finally, because the human studies only considered respiratory perturbations, we divided the analyses into two groups: Studies 1–2, which considered hemorrhage, fluid resuscitation, and respiratory perturbations in pigs, and Studies 3–5, which only considered respiratory perturbations in humans.

Study 1 considered severe hemorrhage (65% of the total blood volume), fluid resuscitation (25%), and respiratory perturbations, and reported the values of four vital signs (Figure 2; MAP, HR, ETCO2, and SpO2). Thus, we compared the CR model predictions with the reported values for these vital signs. The CR model yielded relatively small RMSEs for MAP (18.44 mm Hg), ETCO2 (4.95 mm Hg), and SpO2 (0.99%), but a relatively large RMSE for HR (58.05 beats/min) compared to the corresponding experimental values (Table 2). In general, it is challenging to accurately predict HR dynamics because it is affected by a number of factors, such as pain and level of distress [54-56], which we do not represent in the model. Table 2 also shows the RMSEs of Guyton's model and HumMod. While all three models yielded similar RMSEs for MAP, the RMSEs for the CR model were 3% to 10% smaller for HR, 60% for ETCO2, and 98% for SpO2. During the simulations, the Guyton model's MAP predictions fell outside of the physiological range and its HR predictions changed unrealistically ~9 minutes into the simulation (Figure 2, A and B, respectively), likely caused by its inability to consider respiratory perturbations. In addition, it cannot predict ETCO2 or SpO2. As discussed above, Cheng's model could not simulate the severe hemorrhage condition of Study 1 because it does not account for the fluid-shift mechanism, which compensates for body fluid loss. In terms of prediction accuracy, 71% of the nominal CR model predictions of ETCO2 in Study 1 fell within their respective CIs (Table 2). None of the other three models achieved this accuracy (Table 2).

Study 2 also considered severe hemorrhage (65%), fluid resuscitation (35%), and respiratory perturbations, and reported the values of three vital signs (Figure 3; MAP, HR, and ETCO2). Similar to the results in Study 1, the CR model yielded relatively small RMSEs for MAP and ETCO2, but a relatively large RMSE for HR (Table 2). Yet, the CR model still achieved a considerably better prediction than Guyton's model for HR (a 33% reduction) and a similar prediction for MAP. As in Study 1, Guyton's model predictions of MAP and HR towards the end of the hemorrhage simulation yielded unphysiological results (Figure 3, A and B, respectively). With regard to HumMod, because the entire blood loss occurred within 30 minutes, the computations stopped within the initial hemorrhage simulation period, suggesting that a sudden 65% reduction in total blood volume is outside its nominal simulation limits. In terms of prediction accuracy, none of the four models achieved more than 70% accuracy for any of the predicted vital signs reported in this experimental study (Table 2).

Studies 3–5 considered respiratory perturbations in humans and reported the values of ETCO2, SpO2, and PaO2. When averaged over the three studies, the CR model yielded small RMSEs for ETCO2 (2.94 mm Hg), SpO2 (5.81%), and PaO2 (10.06 mm Hg) (Table 2, Figure 4, and Figures S1 and S2 in the Supplementary Material). Moreover, for these studies, we could only compare the CR model to Cheng's model and HumMod because Guyton's model is a purely cardiovascular model without the ability to predict respiratory vital signs. Both the CR model and Cheng's model yielded very similar errors for all three vital signs. This is not surprising given that the respiratory component in the CR model was adapted from Cheng's model. In contrast, compared to the CR model, HumMod's prediction error was slightly lower for ETCO2 (10%) but considerably larger for SpO2 (22%) and PaO2 (64%). Figure 4 shows the measured data and predictions for Study 3, where all three models correctly captured the trend of the two measured vital signs (ETCO2 and PaO2). However, while all three models yielded equivalent RMSEs for ETCO2, HumMod's error for PaO2 was >33% larger than the other models (Table 2). Similar to Study 2, none of the four models achieved a 70% prediction accuracy for the experimental data reported in Studies 3–5 (Table 2).

3.2. Calibration of the CR Model

We conducted a global sensitivity analysis of the CR model and identified its 10 most sensitive parameters for the four outputs using data from Study 1 (Table S3 in the Supplementary Material). Most of these 10 parameters are associated with the regulation or direct estimation of at least one or more of the four vital signs. Moreover, these 10 parameters were consistently more sensitive than others at greater than 95% of the simulated time points. To reduce prediction errors of the CR model, we first calibrated the values of these 10 most sensitive parameters to match the CR model predictions with the means of the experimental data from Study 1. After calibrating the CR model to Study 1 data, we observed modest reductions in its prediction errors (when compared to the nominal, un-calibrated model) for the Study 1 data: 21% for MAP, 26% for HR, 2% for ETCO2, and 43% for SpO2. In addition, when we used the calibrated CR model to predict the remaining studies (Studies 2–5), we again observed only modest reductions in the prediction errors. For example, Figure 3 shows the results for Study 2, illustrating the measured experimental data along with the CR model predictions before (solid line) and after (dash-dot line) calibration. In this case, the differences between the two predictions were consistently small across the four predicted vital signs, with between-model RMSEs of 6.13 mm Hg for MAP, 17.36 beats/min for HR, 0.62 mm Hg for ETCO2, and 0.32% for SpO2. On average, across Studies 2–5, the calibration of the CR model reduced its prediction errors by 14% for MAP, 18% for HR, 22% for ETCO2, and 16% for SpO2 (Table 2, Figures 2–4, and Figures S1 and S2 in the Supplementary Material). In addition, the calibrated CR also increased the prediction accuracy in four specific cases compared to the nominal CR model, i.e., the ETCO2 prediction in Studies 2–3, SpO2 prediction in Study 1, and PaO2 prediction in Study 3, while it remained unchanged for most other outputs in the studies (Table 2).

Furthermore, because Study 1 reported individual data for each of the nine subjects, we also assessed whether an individualized CR model calibrated for each subject could better capture the inherent variability in the data. To this end, we calibrated the CR model to the data representing the four model outputs for each of the nine subjects, and found that the trends in all model outputs for each of the subjects were not drastically different from those observed with the nominal CR model. Quantitatively, the RMSEs obtained when we used the individually calibrated CR model vs. the nominal CR model to predict the data for each of the nine subjects in Study 1 were, on average, 33% smaller for MAP (19.59 vs. 13.12 mm Hg), 25% smaller for HR

(64.17 vs. 48.00 beats/min), and indistinguishable for ETCO2 (7.70 vs. 7.30 mm Hg) and SpO2 (1.53 vs. 1.51%). However, except for SpO2, the average RMSEs for the other three vital signs (MAP, HR, and ETCO2) obtained with the individualized models were not considerably different from those obtained with the model calibrated to predict the mean response over the nine subjects.

4. DISCUSSION

Given that future military conflicts are expected to be encumbered by evacuation delays and high casualty rates, medics will need to increasingly rely on emerging autonomous and semi-autonomous artificial intelligence technologies to administer prolonged field care. Development and assessment of such technologies necessitate the availability of accurate mathematical models that can replicate the physiological responses of key battlefield injuries, such as hemorrhage and airway compromise, and the associated clinical interventions. Here, we have developed a new mathematical model specifically designed to represent these battlefield injuries by expanding and integrating Guyton's model [30] and Cheng's model [36], both of which have certain limitations that preclude them from fully capturing the response to such injuries. The resulting CR model is better able to simulate severe hemorrhage, fluid resuscitation, and respiratory perturbations, and can predict seven key cardiovascular and respiratory vital signs (MAP, SBP, DBP, HR, ETCO2, SpO2, and PaO2) (Figure 1). The model incorporates both cardiovascular and respiratory dynamics, along with their regulatory mechanisms and couplings.

4.1. CR Model Prediction Performance

To assess the CR model's performance, we compared it with three other models (Guyton, Cheng, and HumMod [44]) using experimental data from five studies, involving pigs and humans. When compared to the other three models, the CR model was the only one capable of generating the time courses of all five reported cardiovascular and respiratory outputs in the five studies (MAP, HR, ETCO2, SpO2, and PaO2). Overall, when weighted equally across all five studies, the nominal CR model yielded small average RMSEs for MAP (20.88 mm Hg), ETCO2 (3.50 mm Hg), SpO2 (3.40%), and PaO2 (10.06 mm Hg), but a relatively large RMSE for HR (70.23 beats/min). We also assessed whether we could improve its performance by calibrating the CR model's 10 most sensitive parameters using data from experimental Study 1. Overall, the

calibrated model reduced the prediction errors in Studies 2–5 by a modest 14% for MAP, 18% for HR, 22% for ETCO2, and 16% for SpO2, suggesting that the CR model was stable and robust to its nominal parameter values. While the four models yielded similar prediction errors for MAP, the RMSEs for the CR model were 3% to 10% smaller than the other models for HR, 11% to 15% for ETCO2, 0% to 33% for SpO2, and 10% to 64% for PaO2. In addition, while none of the models achieved the desired prediction accuracy of 70% of the predictions falling within the CIs, in general, the CR model had a higher prediction accuracy than the other models, and achieved the desired accuracy in three specific cases, i.e., the $ETCO_2$ prediction in Study 3 and the SpO2 prediction in Study 1 when using the calibrated CR model, and the $ETCO_2$ prediction in Study 1 when using the nominal CR model (Table 2). In general, none of the four models could predict HR accurately (Table 2). One possible reason for this could be that even though we know that many factors, such as pain and level of distress, can affect HR dynamics [54-56], the mechanistic relations linking these factors to HR are not established, precluding their incorporation into a mathematical model.

Based on the experimental conditions of the studies, we divided the analyses into two groups: Studies 1–2, which considered severe hemorrhage, fluid resuscitation, and respiratory perturbations in pigs; and Studies 3–5, which only considered respiratory perturbations in humans. For Studies 1–2, the CR model yielded small RMSEs for MAP (20.88 mm Hg), ETCO2 (4.36 mm Hg), and SpO2 (0.99%) (Table 2). Similarly, for Studies 3–5, the CR model yielded small RMSEs for ETCO2 (2.94 mm Hg), SpO2 (5.81%), and PaO2 (10.06 mm Hg) (Table 2). Overall, these results indicate that the CR model performed adequately when compared with experimental data. However, comparing its performance with the other models was challenging. In one instance, for the purely cardiovascular Guyton's model, which does not predict respiratory vital signs, we could only compare a subset of the seven vital signs predicted by the CR model. In addition, due to its inability to account for respiratory perturbations, Guyton's model produced qualitative and quantitative non-physiological predictions during periods of severe blood loss in Studies 1–2 (Figures 2, A and 3, A). Thus, we could only compare its MAP predictions for mild or moderate blood loss and fluid resuscitation, which, on average, yielded a similar accuracy as those of the CR model predictions (RMSE: 20.88 vs. 19.01 mm Hg). At other times, even HumMod and Cheng's model, which can predict all vital signs, were unable to simulate certain

experimental conditions. For example, Cheng's model could not simulate the severe hemorrhage condition in Studies 1–2 because it does not account for the fluid-shift mechanism between the blood and the interstitial fluid, which compensates for changes in blood volume due to hemorrhage or fluid resuscitation. Similarly, the HumMod software could not simulate the acute severe hemorrhage in Study 2 and yielded larger prediction errors than the CR model for MAP (5%), ETCO2 (60%), and SpO2 (98%) in Study 1. It is possible, however, that HumMod's nominal parameter values are not suitable for modeling severe hemorrhage and that changing certain parameter values, such as heart contractility and gain of the sympathetic effects on the HR, could resolve these issues.

For Studies 3–5, compared to the CR model, HumMod's prediction error was slightly smaller for ETCO2 (10%) but considerably larger for SpO2 (22%) and PaO2 (64%). These CR model predictions of respiratory perturbations are encouraging, given its simplicity vis-à-vis the more complex HumMod software. In addition, compared to the CR model, Cheng's model produced similar predictions for SpO2 and PaO2 (Figure 4, D and Figures S1, D and S2, D in the Supplementary Material), while its ETCO2 predictions were different (Figure 4, C and Figures S1, C and S2, C in the Supplementary Material). While we adapted the respiratory component and coupling mechanisms between the respiratory and cardiovascular components from Cheng's model, we had to simplify some of the coupling equations to match the reduced number of cardiovascular compartments in the CR model. It is possible that this simplification process affected the ETCO2 predictions of the CR model (ETCO2 was highly sensitive to two vein-related parameters of the cardiovascular component) and potentially led to the differences in its predictions compared to Cheng's model. In contrast, PaO2 was not sensitive to any model parameter of the cardiovascular component and, accordingly, we did not see a large variation in its predictions between the two models. Unfortunately, Studies 3–5 only reported measurements of respiratory vital signs, which prevented us from quantitatively assessing the models' performance for MAP and HR against the experimental data in these studies, but we compared these predictions across the models. Interestingly, while MAP and HR predictions were quantitatively different across the three models (Figure 4, A and B, and Figures S1, A and B, and S2, A and B, in the Supplementary Material), we observed similar qualitative trends for both MAP and HR in the CR model and Cheng's model. However, in HumMod they appeared to be

insensitive to respiratory perturbation. We believe that the different implementation of the cardiovascular component in the three models could have led to the differences in their MAP and HR predictions.

We also investigated whether calibrating the CR model to a specific experimental dataset would increase its prediction accuracy. To avoid overfitting, we only calibrated a subset of 10 parameters that the four outputs were most sensitive to, as determined by a global sensitivity analysis (Table S3 in the Supplementary Material). While the calibration procedure only modestly improved CR model performance, the sensitivity analysis provided insight into which subsystems might be critical for the regulation and maintenance of different outputs. For example, in the CR model, the cardiovascular vital signs MAP and HR were primarily governed by four mechanisms, including the fluid shift from the interstitial fluid, the renal system, the sympathetic stimulation, and the angiotensin mechanism. Yet, interestingly, MAP outputs consistently showed higher sensitivities to parameters representing gains associated with the interstitial fluid (k_{fs}), the renal system (k_{Sk}), and the sympathetic stimulation (k_{SR}), but not the angiotensin system, indicating that the influence of this system on MAP may not be as strong as the others. Moreover, the HR output, which is strongly coupled with MAP [57], was also sensitive to parameters representing gains associated with the interstitial fluid (k_{fs}) and the sympathetic stimulation (HR_2) [Equation (S32) in the Supplementary Material], but not to the two other mechanisms. On the other hand, the respiratory vital signs were primarily governed by the mechanisms of gas storage and exchange between the blood and the three other compartments, i.e., the lungs, the brain tissue, and the body tissue (Figure 1, C). Interestingly, the respiratory output ETCO2 was sensitive to only one of the parameters representing a respiratory mechanism [the metabolic rate of CO_2 (M_{dCO2})] and, in fact, was more sensitive to two specific vein-related cardiovascular parameters [the initial venous volume (V_{v0}) and the compliance of veins (C_v)]. Performing this sensitivity analysis allowed us to understand and quantify the dependencies of the respiratory outputs on the cardiovascular parameters and further highlight the importance of incorporating the coupling mechanism between the cardiovascular and respiratory systems to accurately capture the responses of battlefield trauma.

Given that hemorrhage and airway compromise are the leading causes of potentially survivable death on the battlefield [7], we specifically developed the CR model to account for these two injury modalities. To this end, in modeling the cardiovascular and respiratory systems, we specifically attempted to capture the responses of hemorrhage, fluid resuscitation, and respiratory perturbations, which resulted in more accurate predictions than three other existing models with similar and much higher complexities. However, it is important to note that the existing cardiovascular and respiratory models were developed for predicting different endpoints than the CR model. For example, Guyton's model focused exclusively on circulatory hemodynamics, while Cheng's model was developed to study the effects of hypoxia-induced breathing, chronic heart failure, and obstructive sleep apnea on the cardiovascular and respiratory systems. In addition, even though the CR model performed relatively better than the existing models, its predictive accuracy would be potentially improved. For example, as a starting point, the following four modifications, listed in order of highest to lowest impact on accuracy, could potentially improve the CR model's performance in the future. *1*) Incorporation of the regulatory effects of other subsystems currently not present in the model, such as the endocrine and immune systems [58, 59], would certainly improve the CR model's fidelity. Currently, we only account for the interdependencies between the cardiovascular and respiratory outputs and two critical systems, i.e., the autonomic nervous system and the renal system. *2*) We could explicitly model the effect of emotional stressors, such as pain, anxiety, and fear, on different subsystems in the body. There is ample evidence in the literature that pain activates the sympathetic nervous system [54-56, 60] and the endocrine system [61], leading to an acceleration in HR, an increase in contractility and tone of the heart walls, an elevation in MAP, and the release of hormones, such as cortisol, renin, angiotensin, and aldosterone. Therefore, incorporating such effects could potentially reduce the discrepancies between the CR model predictions and the experimental data, improving model accuracy. *3*) In the current CR model, we used only four outputs (MAP, HR, ETCO2, and SpO2) provided in the experimental studies to calibrate the model parameters. However, there are experimental studies that also report measurements of intermediate cardiovascular and respiratory outputs, such as PaO2, PaCO2, urine rate, O_2 consumption, and CO_2 production during trauma [62]. As more data become available, we could potentially use the values of these intermediate variables along with the four outputs to calibrate the CR model parameters and improve its prediction accuracy. *4*) If we could obtain real-time measurements of

the different vital signs during hemorrhage and resuscitation, we could potentially use a Kalman filter algorithm [63] to reduce the prediction errors of the CR model. Specifically, we could use the CR model to predict the vital signs, compute the estimation errors against the measured values, and use the Kalman filter to update specific CR model parameter values in real time to reduce the estimation errors, thus increasing the model's prediction accuracy.

It is noteworthy, however, that not all of the modifications we mentioned above are currently achievable right away. In terms of feasibility, we believe it would be possible to perform modifications *3* and *1* first. Modification *3* is the most feasible as more data become available. We believe that it can help us better calibrate the model parameters and thus improve model prediction accuracy. Furthermore, with regards to modification *1*, while increasing the model complexity by adding more physiological subsystems currently not represented in the model will improve model fidelity, we need to be careful about only adding components that are absolutely necessary to capture trauma. As is evidenced in our analysis, increased complexity does not always translate into increased accuracy. For example, HumMod has over 5,000 parameters and variables, and represents numerous subsystems that are absent in the CR model, yet its accuracy is either similar to or worse than the CR model. We believe that carefully selecting which parameters to add and calibrating the model to hemorrhage and resuscitation experimental data after each addition might improve model accuracy. In contrast, we do not believe that modification *2* is currently achievable because we lack sufficient quantitative information other than heuristics [64], regarding the mechanisms by which pain and other related stressors modify the autonomic and other subsystems in the body, especially during trauma. However, as a first step, we could investigate whether the use of such heuristics to drive the sympathetic nervous system could help us identify the mechanisms in the cardiovascular and respiratory components of the model most affected by pain and to determine what kind of quantitative data we would need to fully implement this modification. Lastly, with regards to modification *4*, using a Kalman filter to update model parameters in real time is only implementable when we have real-time measurements for a subject whose vital-sign changes we are trying to predict under traumatic conditions. However, for off-line predictive purposes, such as the CR model, this approach is not feasible.

We believe that the CR model presented here represents a promising first step to support the development of autonomous or semi-autonomous decision-support and control systems to aid medic care for trauma casualties on the battlefield. With the improvements proposed above, we believe that the CR model could be used to simulate human responses to trauma-induced injuries typical of battlefield scenarios [7]. In particular, the CR model could be used to generate a large synthetic database of virtual trauma casualties by simulating individuals with varying weight, heart contractility, resting vital signs, and rates of hemorrhage and fluid resuscitation to train deep neural network algorithms to aid in field triage and identification of life-saving interventions [8-13]. Likewise, the model could be used to compare and contrast the efficacy of emerging closed-loop control technologies [14-20].

4.2. Assumptions and Limitations

The CR model has several limitations arising from simplifying assumptions. First, for fluid resuscitation, the model accounts for volumetric fluid injection without considering fluid type. In the future, we could accommodate this limitation by calibrating the model for different fluid types. Second, in our validation analyses, we assumed that hemorrhage, fluid resuscitation, and respiratory perturbations have similar effects on humans and pigs. While we developed the CR model for humans, the lack of clinical data forced us to use animal data in certain assessments. However, by normalizing the experimental inputs as well as the simulated outputs, to some extent we accounted for this limitation. Third, as discussed above, we did not model the effect of emotional stressors, such as pain, anxiety, and fear, on the different subsystems represented in our model. While these are important factors that are reflected in the vital signs, we currently lack the needed mechanistic information to model them. Lastly, the CR model did not represent all the different physiological subsystems, including the endocrine system and the immune system [58, 59], because we do not have the data on how these systems affect the vital signs.

5. CONCLUSION

In summary, we specifically developed and assessed a moderately complex mathematical model to predict the responses of the cardiovascular and respiratory systems to battlefield trauma. The CR model demonstrated benefits compared to both similar (Guyton and Cheng) and more

complex (HumMod) models, showing great potential for simulating hemorrhage and airway compromise, the leading causes of battlefield injury.

Conflict of Interest Statement

The authors declare the absence of any commercial or financial relationships that could be construed as a potential conflict of interest.

Disclaimer

The opinions and assertions contained herein are the private views of the authors and are not to be constructed as official or as reflecting the views of the U.S. Army, the U.S. Department of Defense, or The Henry M. Jackson Foundation (HJF) for the Advancement of Military Medicine, Inc. This paper has been approved for public release with unlimited distribution.

Author Contributions

All authors designed the study. XJ, SL, and SN developed the model, and all authors assessed the model results. XJ and JR drafted the manuscript. All authors reviewed the manuscript and approved the submitted version.

Data Availability Statement

All data will be published with the paper.

Funding

We acknowledge support from the U.S. Army Medical Research and Development Command. The HJF was supported under Contract No. W81XWH20C0031.

Acknowledgments

We thank Maria Kuhrmann for her editorial assistance.

REFERENCES

1. Kotmal RS, Scott LL, Janak JC, Tarpey BW, Howard JT, Mazuchowski EL, et al. The effect of prehospital transport time, injury severity, and blood transfusion on survival of US military casualties in Iraq. *J Trauma Acute Care Surg*. 2018; 85:S112-21.
2. Howard JT, Kotwal RS, Santos-Lazada AR, Martin MJ, Stockinger ZT. Reexamination of a battlefield trauma golden hour policy. *J Trauma Acute Care Surg*. 2018; 84:11-8.
3. Maddry JK, Perez CA, Mora AG, Lear JD, Savell SC, Bebarta VS. Impact of prehospital medical evacuation (MEDEVAC) transport time on combat mortality in patients with non-compressible torso injury and traumatic amputations: a retrospective study. *Mil Med Res*. 2018; 5:1-8.
4. Dolan CP, Valerio MS, Childers WL, Goldman SM, Dearth CL. Prolonged field care for traumatic extremity injuries: defining a role for biologically focused technologies. *NPJ Regen Med*. 2021; 6:1-4.
5. Rasmussen TE, Baer DG, Cap AP, Lein BC. Ahead of the curve: sustained innovation for future combat casualty care. *J Trauma Acute Care Surg*. 2015; 79:S61-4.
6. Davis M. Personal communication with the Director of the U.S. Army Combat Casualty Care Program Area Directorate, Fort Detrick, Maryland. 2019.
7. Eastridge BJ, Mabry RL, Seguin P, Cantrell J, Tops T, Uribe P, et al. Death on the battlefield (2001-2011): implications for the future of combat casualty care. *J Trauma Acute Care Surg*. 2012; 73(Suppl 5):S431-7.
8. Liu J, Khitrov MY, Gates JD, Odom SR, Havens JM, Moya MAD, et al. Automated analysis of vital signs to identify patients with substantial bleeding before hospital arrival: a feasibility study. *Shock*. 2015; 43:429-36.
9. Weintraub WS, Fahed AC, Rumsfeld JS. Translational medicine in the era of big data and machine learning. *Circ Res*. 2018; 123:1202-4.
10. Fernandes M, Vieira SM, Leite F, Palos C, Finkelstein S, Sousa JMC. Clinical decision support systems for triage in the Emergency Department using intelligent systems: a review. *Artif Intell Med*. 2020; 102:101762.
11. Ngiam KY, Khor IW. Big data and machine learning algorithms for health-care delivery. *Lancet Oncol*. 2019; 20:e262-73.

12. Maurer LR, Bertsimas D, Bouardi HT, El Hechi M, El Moheb M, Giannoutsou K, et al. Trauma outcome predictor: an artificial intelligence interactive smartphone tool to predict outcomes in trauma patients. *J Trauma Acute Care Surg*. 2021; 91:93-9.
13. Kang DY, Cho KJ, Kwon O, Kwon JM, Jeon KH, Park H, et al. Artificial intelligence algorithm to predict the need for critical care in prehospital emergency medical services. *Scand J Trauma Resusc Emerg Med*. 2020; 28:17.
14. Kramer GC, Kinsky MP, Prough DS, Salinas J, Sondeen JL, Hazel-Scerbo ML, et al. Closed-loop control of fluid therapy for treatment of hypovolemia. *J Trauma*. 2008; 64(Suppl):S333-41.
15. Rinehart J, Lee C, Canales C, Kong A, Kain Z, Cannesson M. Closed-loop fluid administration compared to anesthesiologist management for hemodynamic optimization and resuscitation during surgery: an in vivo study. *Anesth Analg*. 2013; 117:1119-29.
16. Rinehart J, Lilot M, Lee C, Joosten A, Huynh T, Canales C, et al. Cannesson M. Closed-loop assisted versus manual goal-directed fluid therapy during high-risk abdominal surgery: a case-control study with propensity matching. *Crit Care*. 2015; 19:94.
17. Marques NR, Ford BJ, Khan MN, Kinsky M, Deyo DJ, Mileski WJ, et al. Automated closed-loop resuscitation of multiple hemorrhages: a comparison between fuzzy logic and decision table controllers in a sheep model. *Disaster Mil Med*. 2017; 3:1.
18. Jin X, Kim CS, Dumont GA, Ansermino JM, Hahn JO. A semi-adaptive control approach to closed-loop medication infusion. *Int J Adapt Control*. 2017; 32:240-54.
19. Jin X, Bighamian R, Hahn JO. Development and in silico evaluation of a model-based closed-loop fluid resuscitation control algorithm. *IEEE Trans Biomed Eng*. 2019; 66:1905-14.
20. Liu NT, Salter MG, Khan MN, Branson RD, Enkhbaatar P, Kramer GC, et al. Closed-loop control of FiO2 rapidly identifies need for rescue ventilation and reduces ARDS severity in a conscious sheep model of burn and smoke inhalation injury. *Shock*. 2017; 47:200-7.
21. Soller B, Smith C, Zou F, Ellerby GEC, Prince MD, Sondeen JL. Investigation of noninvasive muscle pH and oxygen saturation during uncontrolled hemorrhage and resuscitation in swine. *Shock*. 2014; 42:44-51.
22. Dubin A, Murias G, Estenssoro E, Canales H, Sottile P, Badie J, et al. End-tidal CO_2 pressure determinants during hemorrhagic shock. *Intensive Care Med*. 2000; 26:1619-23.

23. Ursino M, Magosso E. Acute cardiovascular response to isocapnic hypoxia. I. A mathematical model. *Am J Physiol Heart Circ Physiol*. 2000; 279:H149-65.
24. Ursino M, Magosso E. Acute cardiovascular response to isocapnic hypoxia. II. Model validation. *Am J Physiol Heart Circ Physiol*. 2000; 279:H166-75.
25. Magosso E, Ursino M. A mathematical model of CO_2 effect on cardiovascular regulation. *Am J Physiol Heart Circ Physiol*. 2001; 281:H2036-52.
26. Neal ML, Bassingthwaighte JB. Subject-specific model estimation of cardiac output and blood volume during hemorrhage. *Cardiovasc Eng*. 2007; 7:97-120.
27. Olufsen MS, Ottesen JT, Tran HT, Ellwein LM, Lipsitz LA, Novak V. Blood pressure and blood flow variation during postural change from sitting to standing: model development and validation. *J Appl Physiol.* 2005; 99:1523–37.
28. Carlson DE, Kligman MD, Gann DS. Impairment of blood volume restitution after large hemorrhage: a mathematical model. *Am J Physiol Regul Integr Comp Physiol*. 1996; 270:R1163-77.
29. Bighamian R, Parvinian B, Scully CG, Kramer G, Hahn J-O. Control-oriented physiological modeling of hemodynamic responses to blood volume perturbation. *Control Eng Pract*. 2018; 73:149-60.
30. Guyton AC. *Circulatory Physiology III: Arterial Pressure and Hypertension.* Philadelphia, PA: W.B. Saunders Company; 1980.
31. Chiari L, Avanzolini G, Ursino M. A comprehensive simulator of the human respiratory system: validation with experimental and simulated data. *Ann Biomed Eng*. 1997; 25:985-99.
32. Anderson JC, Babb AL, Hlastala MP. Modeling soluble gas exchange in the airways and alveoli. *Ann Biomed Eng*. 2003; 31:1402-22.
33. Wolf MB, Garner RP. A mathematical model of human respiration at altitude. *Ann Biomed Eng*. 2007; 35:2003-22.
34. Kim CS, Ansermino JM, Hahn JO. A comparative data-based modeling study on respiratory CO_2 gas exchange during mechanical ventilation. *Front Bioeng Biotechnol*. 2016; 4:8.
35. Ursino M, Magosso E, Avanzolini G. An integrated model of the human ventilatory control system: the response to hypercapnia. *Clin Physiol*. 2001; 21:447-64.

36. Cheng L, Ivanova O, Fan H-H, Khoo MCK. An integrative model of respiratory and cardiovascular control in sleep-disordered breathing. *Respir Physiol Neurobiol*. 2010; 174:4-28.
37. Lu K, Clark Jr JW, Ghorbel FH, Ware DL, Bidani A. A human cardiopulmonary system model applied to the analysis of the Valsalva maneuver. *Am J Physiol Heart Circ Physiol*. 2001; 281:H2661-79.
38. Trenhago PR, Fernandes LG, Müller LO, Blanco PJ, Feijóo RA. An integrated mathematical model of the cardiovascular and respiratory systems. *Int J Numer Method Biomed Eng*. 2016; 32:e02736.
39. Das A, Camporota L, Hardman JG, Bates DG. What links ventilator driving pressure with survival in the acute respiratory distress syndrome? A computational study. *Respir Res.* 2019; 20:1-10.
40. Fink M, Batzel JJ, Kappel F. An optimal control approach to modeling the cardiovascular-respiratory system: an application to orthostatic stress. *Cardiovasc* Eng: Int J. 2004; 4:27-38.
41. Ellwein LM, Pope SR, Xie A, Batzel JJ, Kelley CT, Olufsen MS. Patient-specific modeling of cardiovascular and respiratory dynamics during hypercapnia. *Math Biosci.* 2013; 241:56-74.
42. Sarmiento CA, Hernández AM, Serna LY, and Mañanas MÁ. An integrated mathematical model of the cardiovascular and respiratory response to exercise: model-building and comparison with reported models. *Am J Physiol Heart Circ Physiol*. 2021; 320:H1235-60.
43. Bray A, Webb JB, Enquobahrie A, Vicory J, Heneghan J, Hubal R, et al. Pulse Physiology Engine: an open-source software platform for computational modeling of human medical simulation. *SN Compr Clin Med*. 2019; 1:362-77.
44. Abram SR, Hodnett BL, Summers RL, Coleman TG, Hester RL. Quantitative circulatory physiology: an integrative mathematical model of human physiology for medical education. *Adv Physiol Educ*. 2007; 31:202-10.
45. Hall J, Hall M. *Guyton and Hall Textbook of Medical Physiology.* New York, NY: Elsevier; 2021.

46. Herff H, Paal P, von Goedecke A, Lindner KH, Severing AC, Wenzel V. Influence of ventilation strategies on survival in severe controlled hemorrhagic shock. *Crit Care Med*. 2008; 36:2613-20.
47. Reynolds WJ, Milhorn Jr, HT. Transient ventilatory response to hypoxia with and without controlled alveolar PCO_2. *J Appl Physiol*. 1973; 35:187-96.
48. Martinoni EP, Pfister CA, Stadler KS, Schumacher PM, Leibundgut D, Bouillon T, et al. Model-based control of mechanical ventilation: design and clinical validation. *Br J Anaesth*. 2004; 92:800-7.
49. Easton PA, Anthonisen NR. Ventilatory response to sustained hypoxia after pretreatment with aminophylline. *J Appl Physiol*. 1988; 64:1445-50.
50. Walpole SC, Prieto-Merino D, Edwards P, Cleland J, Stevens G, Roberts I, et al. The weight of nations: an estimation of adult human biomass. *BMC Public Health*. 2012; 12:439.
51. Altman DG, Bland JM. Interaction revisited: the difference between two estimates. *BMJ*. 2003; 326:219.
52. Priezjev NV, Vital-Lopez FG, Reifman J. Assessment of the unified model of performance: accuracy of group-average and individualised alertness predictions. *J Sleep Res*. 2022; 13626.
53. Helton JC, Davis FJ. Latin hypercube sampling and the propagation of uncertainty in analyses of complex systems. *Reliab Eng Syst Saf*. 2003; 81:23-69.
54. Zubrzycki M, Liebold A, Skrabal C, Reinelt H, Ziegler M, Perdas E, et al. Assessment and pathophysiology of pain in cardiac surgery. *J Pain Res.* 2008; 11:1599-611.
55. Tovote P, Meyer M, Pilz PK, Ronnenberg A, Ögren SO, Spiess J, et al. Dissociation of temporal dynamics of heart rate and blood pressure responses elicited by conditioned fear but not acoustic startle. *Behav Neurosci*. 2005; 119:55.
56. Tousignant-Laflamme Y, Rainville P, Marchand S. Establishing a link between heart rate and pain in healthy subjects: a gender effect. *J Pain*. 2005; 6:341-7.
57. Abbott TE, Pearse RM, Archbold RA, Ahmad T, Niebrzegowska E, Wragg A, et al. A prospective international multicentre cohort study of intraoperative heart rate and systolic blood pressure and myocardial injury after noncardiac surgery: results of the VISION study. *Anesth Analg*. 2018; 126:1936.

58. Rhee SS, Pearce EN. The endocrine system and the heart: a review. *Rev Esp Cardiol*. 2011; 64:220-31.
59. Hinghofer-Szalkay HC. Physiology of cardiovascular, respiratory, interstitial, endocrine, immune, and muscular systems. In: *Biological and Medical Research in Space*. Berlin: Springer; 1996, p. 107-53.
60. Sacco M, Meschi M, Regolisti G, Detrenis S, Bianchi L, Bertorelli M, et al. The relationship between blood pressure and pain. *J Clin Hypertens*. 2013; 15:600-5.
61. Tennant F. The physiologic effects of pain on the endocrine system. *Pain Ther*. 2013; 2:75-86.
62. Kheirabadi BS, Arnaud F, McCarron R, Murdock AD, Hodge DL, Ritter B, et al. Development of a standard swine hemorrhage model for efficacy assessment of topical hemostatic agents. *J Trauma Acute Care Surg*. 2011; 71:S139-46.
63. Bishop G, Welch G. *An Introduction to the Kalman Filter* (SIGGRAPH 2001, Course 8). New York: Association for Computing Machinery; 2001, p. 41.
64. Terkelsen AJ, Mølgaard H, Hansen J, Andersen OK, Jensen TS. Acute pain increases heart rate: differential mechanisms during rest and mental stress. *Auton Neurosci*. 2005; 121:101-9.

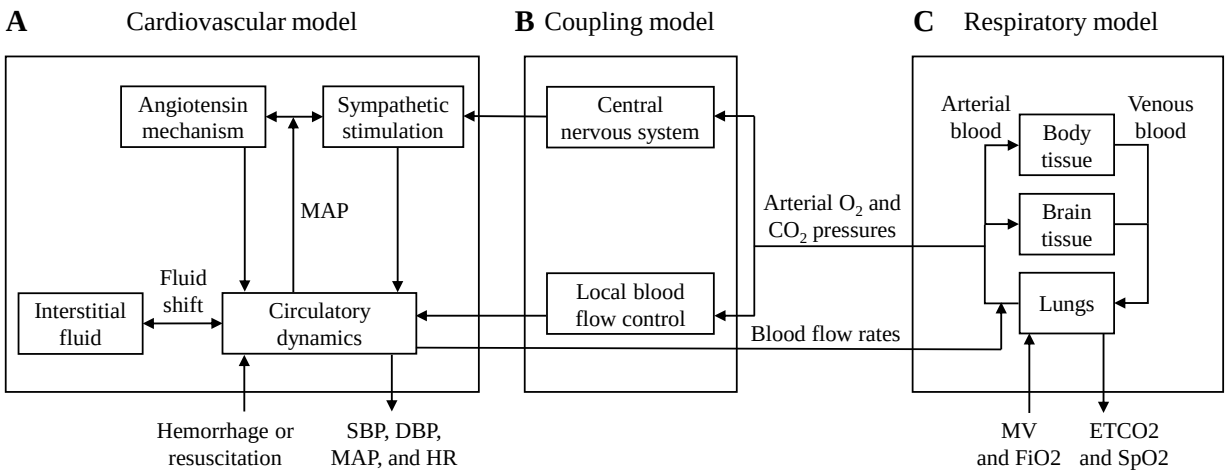

Figure 1. Schematic block diagram of the cardio-respiratory (CR) model. The CR model consists of a cardiovascular model (A), coupling model (B), and respiratory model (C). A) The cardiovascular model includes circulatory dynamics, the fluid shift between the circulatory and interstitial fluid compartments, sympathetic stimulation, and the angiotensin control mechanism. The model's inputs are the rates of hemorrhage or fluid resuscitation, and the outputs consist of four cardiovascular vital signs, systolic blood pressure (SBP), diastolic blood pressure (DBP), mean arterial pressure (MAP), and heart rate (HR). B) The coupling model describes how the cardiovascular and respiratory models interact via the central nervous system and local blood flow control. C) The respiratory model consists of three compartments, representing gas storage and exchange in the lungs, brain tissue, and body tissue. The model's inputs are the minute ventilation (MV) and the fraction of inspired oxygen (FiO2), and its outputs consist of the partial pressure of end-tidal carbon dioxide (ETCO2) and oxygen saturation (SpO2).

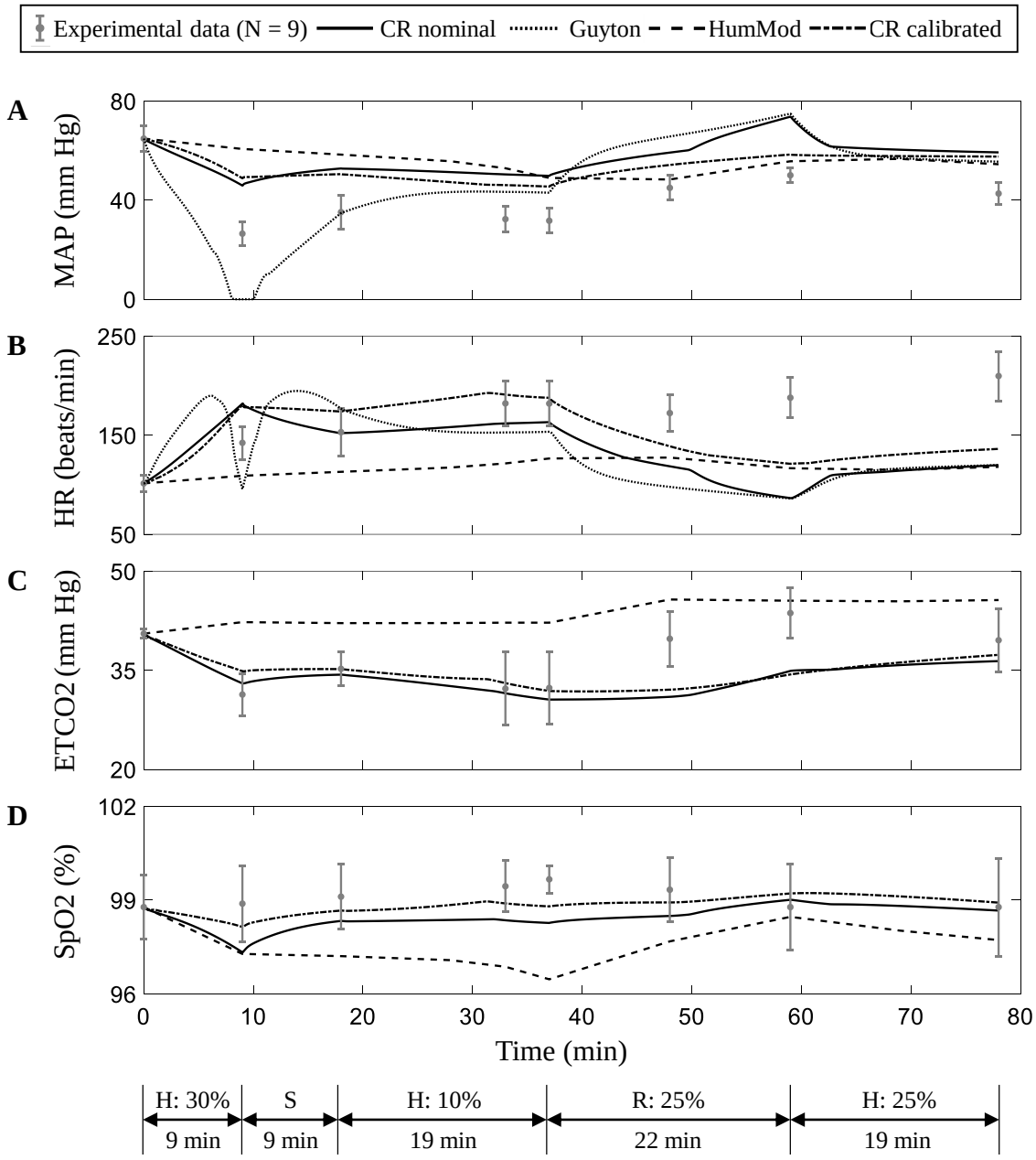

Figure 2. Comparison between Study 1 experimental data, simulated outputs for the cardio-respiratory (CR) model using nominal (solid line) and calibrated (dash-dot line) model parameters, and simulated outputs for Guyton's model (dotted line) and HumMod (dashed line). A) Mean arterial pressure (MAP). B) Heart rate (HR). C) End-tidal carbon dioxide (ETCO2). D) Oxygen saturation (SpO2). H and R represent the volumetric fraction of hemorrhage and fluid resuscitation, respectively, of total blood volume. S represents the period where hemorrhage was stopped but no fluid resuscitation was provided. Gray dots represent mean experimental data (error bars denote two standard errors of the mean; N = 9). Throughout the study, the minute ventilation and fraction of oxygen were adjusted to maintain an ETCO2 of ~40 mm Hg.

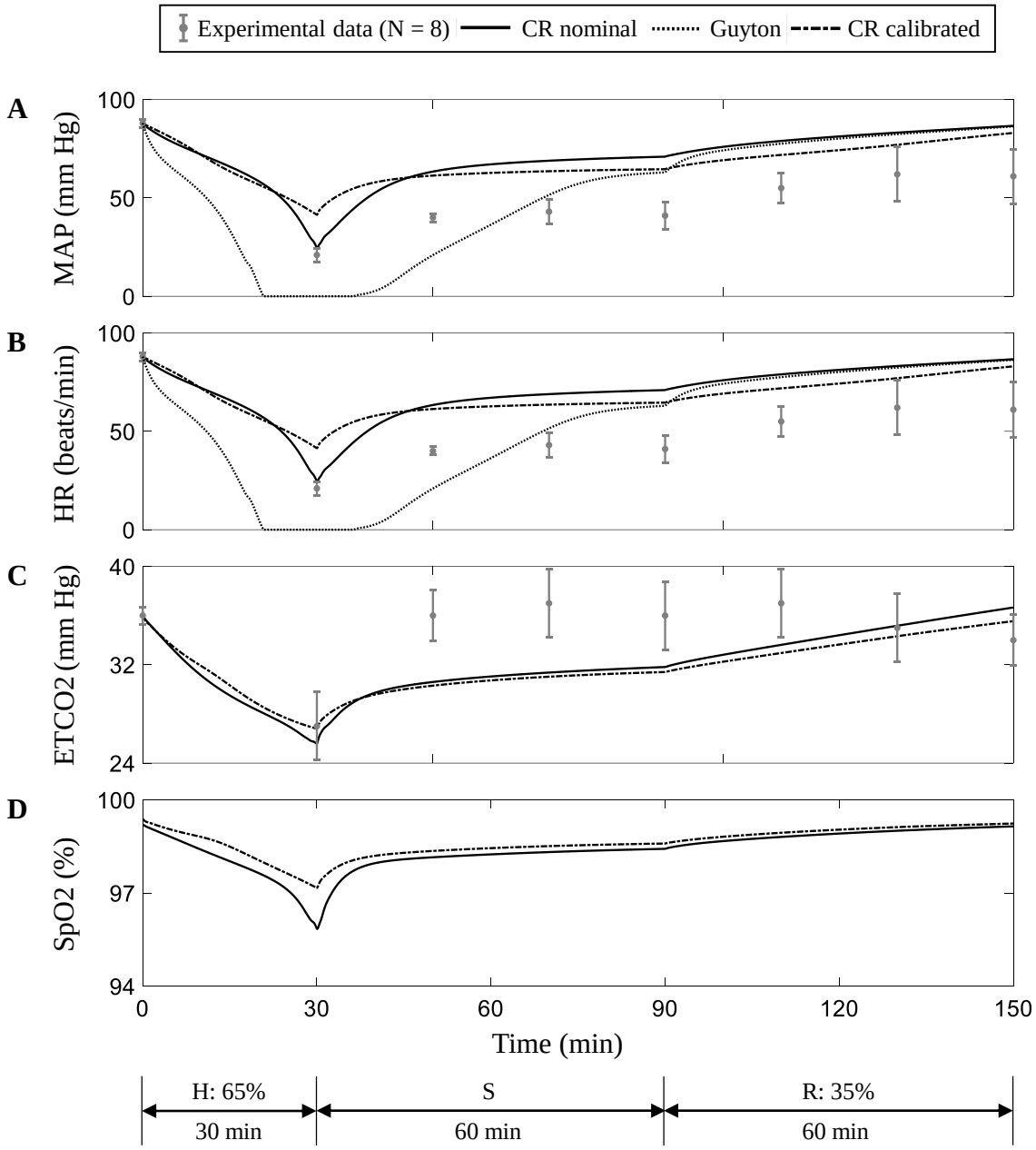

Figure 3. Comparison between Study 2 experimental data, simulated outputs for the cardio-respiratory (CR) model using nominal (solid line) and calibrated (dash-dot line) model parameters, and simulated outputs for Guyton's model (dotted line). A) Mean arterial pressure (MAP). B) Heart rate (HR). C) End-tidal carbon dioxide ($ETCO_2$). D) Oxygen saturation (SpO_2). H and R represent the volumetric fraction of hemorrhage and fluid resuscitation, respectively, of total blood volume. S represents the period where hemorrhage was stopped but no fluid resuscitation was provided. Gray dots represent mean experimental data (error bars denote two standard errors of the mean; N = 8). Throughout the study, the fraction of oxygen was set to be 100% and the minute ventilation was adjusted to maintain an ETCO2 of 35–45 mm Hg.

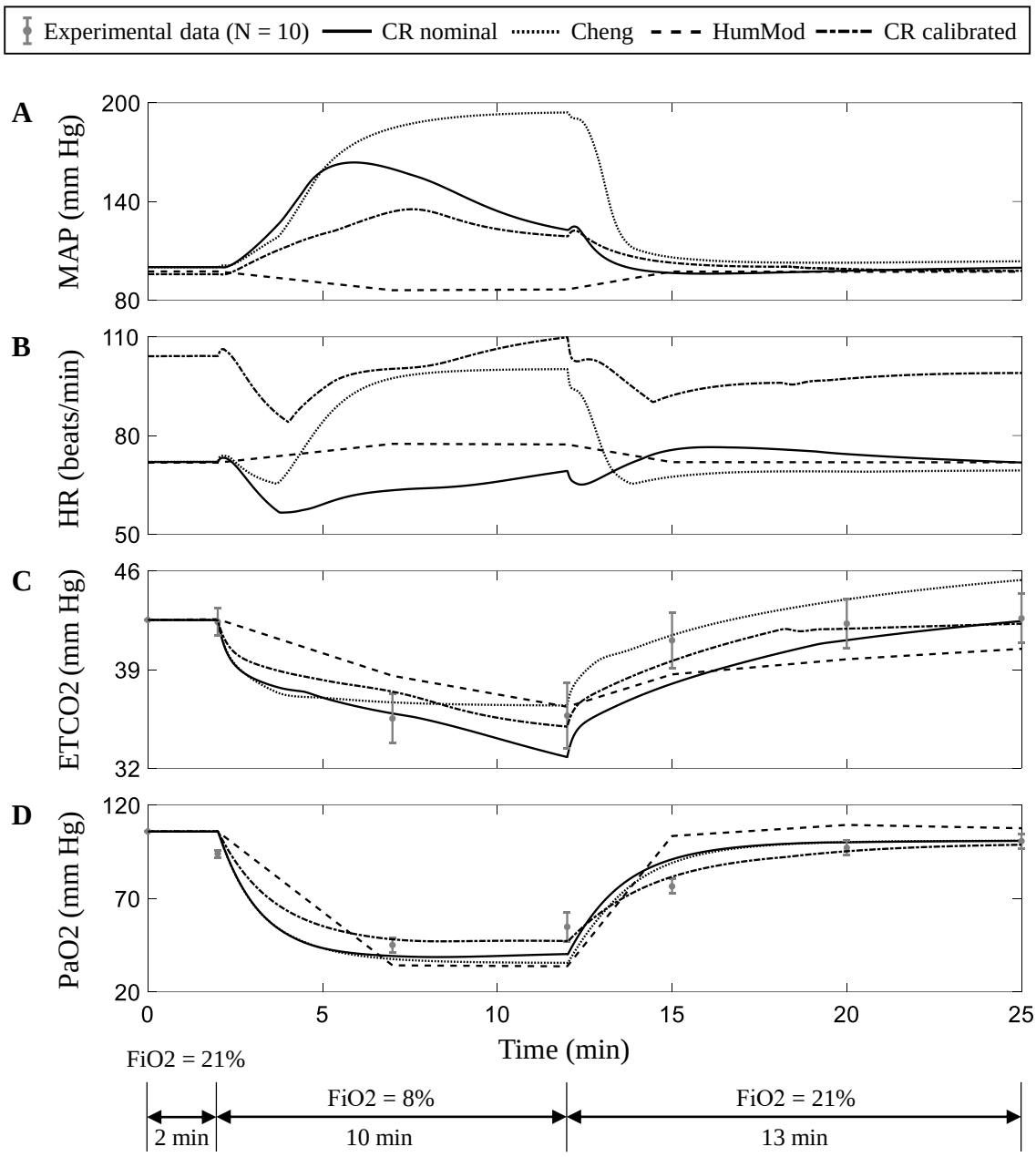

Figure 4. Comparison between Study 3 experimental data, simulated outputs for the cardio-respiratory (CR) model using nominal (solid line) and calibrated (dash-dot line) model parameters, and simulated outputs for Cheng's model (dotted line) and HumMod (dashed line). A) Mean arterial pressure (MAP). B) Heart rate (HR). C) End-tidal carbon dioxide (ETCO2). D) Arterial oxygen pressure (PaO2). FiO2 represents the fraction of inspired oxygen. Gray dots represent mean experimental data (error bars denote two standard errors of the mean; N = 10). Throughout the study, human participants controlled the minute ventilation spontaneously.

Table 1. Experimental studies used for comparing the four models and calibrating the cardio-respiratory model

Study	# of subjects	Species	Age (yrs)	Weight (kg)	Duration (min)	Hemorrhage amount (%)	Fluid resuscitation amount (%)	MV (L/min)	FiO2 (%)	Reported outputs	Source
Hemorrhage, fluid resuscitation, and respiratory perturbations											
1	9	Pig	-	36–43	78	30–10–25	25	4.4–12.8	26–34	MAP, HR, ETCO2, SpO2	[21]
2	8	Pig	-	35–45	150	65	35	3.5–10.8	100	MAP, HR, ETCO2	[46]
Respiratory perturbations											
3	10	Human	22–29	-	25	-	-	3.5–15.0	9–21	ETCO2, PaO2	[47]
4[a]	16	Human	20–59	54–87	30	-	-	6.0–9.0	21	ETCO2	[48]
5[a]	20	Human	26[b]	-	34	-	-	6.6–12.0	12–21	ETCO2, SpO2	[49]

[a]Studies 4–5 only provided experimental data for one subject.
[b]Average age.
ETCO2: end-tidal carbon dioxide; FiO2: fraction of inspired oxygen; HR: heart rate; MAP: mean arterial pressure; MV: minute ventilation; PaO2: arterial O_2 pressure; SD: standard deviation; SpO2: oxygen saturation.

Table 2. Root mean square errors (RMSEs) between model predictions and experimental data, and percentage of model predictions that fell within the confidence intervals of the experimental data for the five studies

Study	# of subjects	Cardio-respiratory (CR)				Guyton		Cheng		HumMod	
		Nominal		Calibrated							
		RMSE	Percentage	RMSE	Percentage	RMSE	Percentage	RMSE	Percentage	RMSE	Percentage
Mean arterial pressure (mm Hg)											
1	9	18.44	0	14.60	0	17.58	14	*	*	19.32	14
2	8	23.32	0	20.16	0	20.44	0	*	*	*	*
Heart rate (beats/min)											
1	9	58.05	43	43.08	43	63.68	14	*	*	59.69	0
2	8	82.41	14	67.43	14	109.70	0	*	*	*	*
End-tidal carbon dioxide (mm Hg)											
1	9	4.95	71	4.84	57	†	†	*	*	7.94	14
2	8	3.76	29	3.94	43	†	†	*	*	*	*
3	10	1.81	67	1.05	83	†	†	1.43	65	2.10	33
4	1	2.27	◊	1.57	◊	†	†,◊	3.56	◊	2.69	◊
5	1	4.73	◊	3.26	◊	†	†,◊	4.76	◊	3.13	◊
Oxygen saturation (%)											
1	9	0.99	57	0.56	86	†	†	*	*	1.96	29
5	1	5.81	◊	4.87	◊	†	†,◊	5.79	◊	7.06	◊
Arterial oxygen pressure (mm Hg)											
3	10	10.06	33	6.36	67	†	†	11.08	27	16.49	0

*The corresponding model was unable to simulate the experimental condition of the study.
†The model does not predict the corresponding output.
◊The corresponding study did not report the standard error of the experimental data.